Permeation of PLGA nanoparticles across different *in vitro* models

Lindiwe A Nkabinde[1], Lungile NN Shoba-Zikhali[1], Boitumelo Semete-Makokotlela[2], Lonji Kalombo[2], Hulda S Swai[2], Rose Hayeshi[2], Thembela K Hillie[3], and Josias H Hamman[4,5*]

[1]Council for Scientific and Industrial Research, Biosciences, P0.O Box 395, Pretoria, 0001, South Africa,

[2]Council for Scientific and Industrial Research, Material Science and Manufacturing, Polymers and Bioceramics, P.O Box 395, Pretoria, 0001, South Africa,

[3]Council for Scientific and Industrial Research, National Centre for Nano-structured Materials, P.O Box 395, Pretoria, 0001, South Africa,

[4]Tshwane University of Technology, Department of Pharmaceutical Sciences, Private Bag X680, Pretoria, 0001, South Africa.

[5]North-West University, Unit for Drug Research and Development, Private Bag X6001, Potchefstroom, 2520, South Africa

Running title: Nanoparticle permeation across *in vitro* models

*Corresponding author:

Josias H Hamman (PhD)

Unit for Drug Research and Development,

Private Bag X6001, Potchefstroom, 2520, South Africa

Email: sias.hamman@nwu.ac.za

Tel: +27 18 299 4035

Fax: +27 18 293 5219

ABSTRACT

Mycobacterium tuberculosis (TB) is one of the leading causes of death and is intensified by HIV co-infection and multidrug resistance. Some of the problems associated with currently available drug treatment for TB are poor permeation and low bioavailability. Many drug delivery systems have indicated improvement in targeted-delivery of various drug molecules and among these, biodegradable and biocompatible polymers such as poly(D,L-lactide-*co*-glycolide) (PLGA) have been shown to enhance intracellular uptake of drug candidates when formulated as nanoparticles. PLGA nanoparticles were prepared by means of a double emulsion solvent evaporation technique and evaluated in terms of size, encapsulation efficiency, surface charge, isoniazid release and *in vitro* transport. The nanoparticles have an average size of 237 nm, and were previously shown to be distributed in several tissues after oral administration without triggering an immune response. This study focussed on the *in vitro* permeation of the PLGA nanoparticles across different membranes and showed that although the nanoparticles are efficiently delivered across the intestinal epithelium, they release encapsulated isoniazid very slowly after being transported. This may improve the treatment efficiency due to continuous release of the isoniazid after effective delivery of the nanoparticulate system across the intestinal epithelium, however, this should be confirmed by future *in vivo* studies.

Keywords: Caco-2, isoniazid, nanoparticles, parallel artificial membrane permeability assay, poly(D,L-lactide-*co*-glycolide), transport

INTRODUCTION

About 9.2 million incidence cases of TB have been reported worldwide [1]. Main factors that contribute to failed therapy include immune compromised patients such as those infected with the human immunodeficiency virus (HIV) especially in Sub-Saharan Africa and the emergence of multi-drug resistance [2]. Despite the availability of highly efficacious treatment for decades, TB remains a major global health problem. To date, combinatorial therapy is still the cornerstone in treatment of *Mycobacterium tuberculosis* infections and even though mono-drug treatment is discouraged due to occurrence of drug resistance, many biologists are interested in the evaluation of hydrophilic drugs, like isoniazid, which play a fundamental role in the second phase of TB treatment. At this second phase of treatment, isoniazid is designated to specifically kill rifampicin–resistant mutant microorganisms that have commenced replication [3] and most importantly destroy dominant *bacilli* that might cause a relapse of the disease [4]. Hence, isoniazid is regarded as one of the most effective drugs in the multi-therapy regimen used against *Mycobacterium tuberculosis* infections [5].

The oral route is still preferred over other drug administration routes, owing to its credential amongst others to optimise factors like bioavailability, pharmacologic effects and toxicity through formulation strategies [6]. However, this advantage is overshadowed by physiological barriers that prevent certain chemical entities from entering the body thus compromising their bioavailability. Such barriers include pre-systemic enzymatic degradation in the gut lumen [7], poor solubility and low permeability [8], the effect of efflux transporters [9, 10] and biliary excretion via enterohepatic shunt process [7].

Numerous drug carriers such as liposomes have been extensively used for drug delivery and targeting. Perhaps, the greatest advantage of using liposomes is that they protect drug molecules against metabolism and lysosomal degradation [11] and also present excellent characteristics of encapsulating both hydrophilic and hydrophobic drugs [12, 13]. However, a rapid release of hydrophilic drugs has been reported for this drug delivery system [14]. To improve on these disadvantages, polymers such as poly(D,L-lactide-*co*-glycolide) (PLGA) and polylactide have entered the world of nanomedicine mainly because they are biocompatible and biodegradable through natural pathways within the Kreb cycle [15]. The United States of America's Food and Drug Administration (FDA) approved these polymers for use in drug delivery systems and they have therefore gained attractiveness for biomedical applications [16-18]. These polymers are used to formulate particulate systems that are designed to protect the drug against enzymatic degradation and to effectively transfer drugs across the gastrointestinal mucosa [19].

This study aimed at evaluating the *in vitro* transport of isoniazid-encapsulated PLGA nanoparticles across artificial membranes and two different Caco-2 cell models. Due to the slow release of isoniazid from these nanoparticles after their transport across the membranes, the transport of Rhodamine 6G-labelled PLGA nanoparticles was also determined to directly measure the permeability of the nanoparticles.

MATERIALS AND METHODS

The following chemicals that were used in the formulation of the nanoparticles were purchased from Sigma-Aldrich (Johannesburg, RSA): 50:50 (poly(D,L-lactide-*co*-glycolide) (PLGA) M_W = 40-75 kDa with an inherent viscosity of 0.57 dl/g), polyvinyl alcohol (PVA, M_W = 13-23 kDa; 87-89% hydrolyzed) ethyl acetate (analytical grade). Isoniazid was generously donated by North West University, South Africa. The Caco-2 cell line was purchased from Highveld Biologicals (Pty) Ltd (Johannesburg, RSA). The growth media and supplements used to maintain cell growth were purchased from Sigma-Aldrich (Johannesburg, RSA), which include Dulbecco's Modified Eagle's Medium (DMEM), Fetal Bovine Serum, penicillin/streptomycin solution, L-glutamine, trypsin/EDTA solution, Hanks Balanced Salt Solution (HBSS), phosphate buffered solution (PBS), D-glucose and 4-(2-hydroxyethyl)-1-piperazineethanesulfonic acid (HEPES). Tissue culture flasks and Transwell™ permeable supports used in the transport studies were supplied by Corning-Costar® (Corning, New York, USA). BIOCOAT® HTS Fibrillar Collagen Multiwell™ Insert System(s), each containing 24 PET membranes (1 μm pore size) with a uniform thin layer of fibrillar collagen and FALCON® 24-well plates used in the 3 day Caco-2 cell transport study as well as 96 well plate used in the parallel artificial membrane permeability assay (PAMPA) were supplied by BD Company (BD Gentest™, California, USA). Reference compounds (viz. atenolol, verapamil and Lucifer yellow) were also purchased from Sigma-Aldrich (St. Louis, Missouri, USA).

Formulation of poly(D,L-lactide-*co*-glycolide) nanoparticles

The PLGA nanoparticles were formulated by means of a double emulsion solvent evaporation method previously described [20]. In summary, 100 mg PLGA was dissolved in 8 ml ethyl acetate. To encapsulate the model drug, 50 mg isoniazid was dissolved in 2 ml PBS adjusted to pH 7.4 thus resulting in a 25 mg/ml isoniazid solution. For encapsulation of Rhodamine 6G, 100 mg PLGA were dissolved in 8 ml ethyl acetate together with 2 mg Rhodamine 6G. To prepare an emulsion, PLGA and isoniazid or Rhodamine 6G solutions were mixed and placed in an ice bath, then homogenised at 5000 rpm for 3 min using a high speed homogenizer (Silverson L4R, Silverson Machines Ltd, UK) to form the first oil-in-water (o/w) emulsion and for the purpose

of reducing the size of the droplets. The first emulsion was then poured into 40 ml of a 1% (w/v) PVA solution, which was homogenised at 8000 rpm for 3 min to form a water-in-oil-in-water (w/o/w) emulsion. This emulsion was stirred overnight on a magnetic stirring plate at 500 rpm to remove the organic solvent through evaporation prior to freeze drying.

The nanoparticles formed through this solvent evaporation procedure were removed by centrifugation at 15000 rpm for 15 min and vortexing three times in between while washing with distilled water. The pellet collected from the centrifugation step was placed at -72 ºC (for a minimum period of 2 h) prior to freeze drying. The particles were lyophilised using a Genesis freeze-dryer (Virtis Co., New York, USA) for 24-48 h.

Encapsulation efficiency

To determine encapsulation efficiency (EE), 2 ml of isoniazid- or Rhodamine 6G-encapsulated PLGA nanoparticles suspension collected from the formulation prior to freeze drying, was centrifuged at 15000 rpm for 2 min at 25 ºC using Beckman Coulter centrifuge (Beckman Coulter Inc., Canada, USA). An aliquot from the supernatant was measured for isoniazid and Rhodamine 6G concentrations using a UV/Vis spectrophotometer at a wavelength of 262 nm and a multimode reader (Infinite F500, Tecan Group Ltd, Männedorf, SC) at 340/485 nm as the excitation/emission wavelengths, respectively. The encapsulation efficiency was then calculated using equation (1) as follows:

$$\text{EE}\ (\%) = \frac{C_s}{C_0} \times 100 \qquad (1)$$

Where C_s is the isoniazid or Rhodamine 6G amount in the isoniazid-encapsulated PLGA nanoparticles or Rhodamine 6G-labelled PLGA nanoparticles as determined by supernatant amount minus initial amount added and C_0 is the initial amount of isoniazid or Rhodamine 6G added in the formulation process [21].

Physical characterisation of nanoparticles

The particle size, polydispersity index (PDI) as well as the zeta potential were determined by means of photon correlation spectroscopy as determined in a Malvern Zetasizer Nano ZS apparatus (Malvern Instruments Ltd, Worcestershire, UK). A quantity of 2 mg of the lyophilised isoniazid-encapsulated PLGA nanoparticles was suspended in 1 ml of distilled water and vortexed for 2 min and introduced into the cell of the Zetasizer apparatus for analysis. The analysis of the nanoparticle sample was performed at 25 °C in triplicate. The surface

morphology of PLGA nanoparticles was analyzed using a scanning electron microscope (LEO 1525 Field Emission scanning electron microscope, Zeiss, Oberkochen, Germany).

Dissolution study

The *in vitro* isoniazid release from the loaded PLGA nanoparticles was determined using a six station dissolution apparatus (TDT-06T, Electrolab, India) with the paddle method. To simulate intestinal fluid pH, the dissolution medium consisted of phosphate buffer, which was prepared by dissolving 68.05 g of KH_2PO4 and 8.96 g of NaOH in distilled water that was made up to a volume of 10 L and adjusted to pH 6.8. Hard gelatin capsules were used to load pure isoniazid powder (immediate release dosage form for comparison) or isoniazid-encapsulated PLGA nanoparticles containing the same weight of isoniazid (calculated by using the encapsulation efficiency), which were placed in the dissolution flasks. The apparatus was operated at 50 rpm and the temperature was maintained at 37 ± 0.5 °C. At time intervals of 0.5, 1, 2, 4, 16 and 24 h samples (5 ml) were collected and immediately replenished by fresh dissolution medium of the same volume to maintain sink conditions. The dissolution samples were filtered through a 0.20 µm membrane and analyzed with an UV/Vis spectrophotometer at a wavelength of 262 nm to determine the isoniazid concentration. The cumulative appearance of the isoniazid released from PLGA nanoparticles was calculated as a percentage of the original amount of isoniazid encapsulated in PLGA nanoparticles. The experiment was carried out in duplicate.

Transport across parallel artificial membranes

The permeability of PLGA nanoparticles encapsulating isoniazid as well as that of Rhodamine 6G-labelled PLGA nanoparticles was determined by the parallel artificial membrane assay (PAMPA) technique in 96 well plates. The permeability was compared with different standard drugs including atenolol (low permeability), verapamil (high permeability) [22] as well as the membrane integrity marker, Lucifer yellow. The plates were equilibrated at 25 ºC for 30 min and then 300 µl of each test compound solution (100 µM for the reference compounds and 100 µg/ml for pure isoniazid and PLGA nanoparticles encapsulating isoniazid) were added to the donor chamber (basolateral side) and 200 µl of PBS were added to the acceptor chamber (apical side). The plates were then incubated at 25 ºC for 5 h after which 100 µl aliquots were collected from the apical chamber and from the basolateral chamber at the end of the experiment and analysed using a UV/Vis spectrophotometer at a wavelength of 220 nm for atenolol and verapamil and at 262 nm for isoniazid containing compounds, while Lucifer yellow and Rhodamine 6G containing samples were analysed by fluorescence spectrofluorometry

(Infinite F500, Tecan Group Ltd, Männedorf, SC) at an excitation/emission wavelength of 485/535 nm and 340/485, respectively. The permeability study was carried out in three independent experiments. The effective permeability (P_e) coefficient values (cm/s) were calculated using equation (2) below, which is deduced from the flux equation as previously described [23].

$$P_e(cm/s) = \frac{-\ln\left[1-C_A(t)/C_{equilibrium}\right]}{A \times (1/V_D + 1/V_A)} \quad (2)$$

Where C_A (t) is the compound concentration in the acceptor chamber at time t (mM), $C_{equilibrium}$ is the concentration when the concentrations of the diffusing compound in the apical and basolateral chambers are equal (assuming the compound is passively permeated). This value is calculated using equation (3) below:

$$C_{equilibrium} = \frac{C_D(t) \times V_D + C_A(t) \times V_A}{(V_D + V_A)} \quad (3)$$

Where C_D (t) is the compound concentration in the donor chamber at time t (mM), V_D is the donor chamber volume (ml), V_A is the acceptor chamber volume (ml), A is the membrane surface area (cm^2), t is the incubation time (s).

Transport across Caco-2 cell monolayers (traditional 21-day culture method)

Caco-2 cells were grown in 75 cm^2 tissue culture flasks (Corning) at 37°C under 5% CO_2 and 90% humidity conditions. They were maintained in sterile Dulbecco's modified eagles medium (DMEM) supplemented with 10% (v/v) heat inactivated Fetal Bovine Serum (FBS), penicillin/streptomycin (100 IU/mL/100 μg/ml) and 2 mM L-glutamine. The cells were propagated with 0.25% trypsin/0.53% EDTA. For the transport studies, Caco-2 cells (passage between 30 and 40) were seeded onto polycarbonate-treated filter membranes in Transwell 12-well plates (0.4 μm pores, 1.12 cm^2 surface area) at a density of 1 x 10^4 cells/ml. The Caco-2 cell monolayer integrity was monitored by the use of transepithelial electrical resistance (TEER) readings over the 21 day growth period until an acceptable reading was obtained indicating a confluent monolayer. To ensure that the cell monolayer was not compromised during transport study, it was washed with PBS and fresh culturing media (DMEM) was added to both apical and basolateral chambers and recovery of TEER value was monitored. The TEER was measured with a Millicell®-ERS meter (Microsep (Pty) Ltd, Johannesburg, RSA) and a measurement of $\geq$ 250 Ω.cm^2 was used as a reference value to indicate the formation of intact monolayers in order to perform the transport studies [24]. The final TEER values were obtained by applying equation (4) as follows:

$$\text{TEER } (\Omega.cm^2) = (T_{\text{with cells}} - T_{\text{w/o cells}}) \times A \quad (4)$$

Where $T_{\text{with cells}}$ is the TEER reading across the filter with cells, $T_{\text{w/o cells}}$ is the TEER reading across the filter without cells and A is the membrane surface area (cm^2) [25].

The integrity of the cell monolayers was further confirmed by transport studies with the Lucifer yellow integrity marker molecule at 10 and 21 days of culturing. This was done by replacing the culture medium of the apical chamber with 100 µl of Lucifer yellow solution at a concentration of 100 µM and the culture medium in the basolateral chamber with 600 µl of transport medium after the cell monolayers were washed three times with phosphate buffer saline. After an hour of incubation, a 200 µl aliquot was removed from the basolateral chamber and analysed by means of fluorescence spectrofluorometry (Tecan Infinite F500, Männedorf, Switzerland) at an excitation wavelength of 485 nm and an emission wavelength of 535 nm. The total percentage rejection of the Lucifer yellow was calculated using equation (5) below:

$$\text{Total rejection } (\%) = [1 - (LY_{Cb} / LY_{Co})] \times 100 \quad (5)$$

Where LY_{Cb} is Lucifer yellow concentration passing through the cell monolayer and LY_{Co} is the initial concentration of the Lucifer yellow.

The transport of PLGA nanoparticles encapsulating isoniazid was compared to that of pure isoniazid in solution across confluent Caco-2 cell monolayers grown on Transwell 12-well membrane inserts. The transport of Rhodamine 6G-labelled PLGA nanoparticles was also compared with pure Rhodamine 6G in solution and with the reference drugs, atenolol and verapamil. The cell monolayers were washed three times with PBS and the cells were then equilibrated with transport medium (HBSS supplemented with 10 mM D-glucose and 10 mM HEPES, pH 7.4). The cell monolayers were then treated with test compounds at 100 µM concentration and maintained at 37 ºC for the entire experiment. The samples were withdrawn from the basolateral side at 0.5, 1, 3, 6 and 24 h (except for reference compounds which were only incubated for 3 h) and analysed using a UV/Vis spectrophotometer at a wavelength of 220 nm for atenolol and verapamil and at 262 nm for isoniazid containing compounds. Lucifer yellow and Rhodamine 6G containing samples were analysed by fluorescence spectrofluorometry (Infinite F500, Tecan Group Ltd, Männedorf, SC) at an excitation/emission wavelength of 485/535 nm and 340/485, respectively. The permeability study was carried out in three independent experiments.

The apparent permeability (P_{app}) coefficient values (cm/s) were calculated using equation (6) below:

$$P_{app}(cm/s) = \frac{dQ}{dt} \times \left(\frac{1}{A.\ C_0}\right) \quad (6)$$

Where dQ/dt is the increase in the amount of drug in the receiver compartment over time or the drug permeation rate (μg/ml/s), A is the surface area of the monolayer (cm^2), and C_0 is the initial concentration of the test compound applied to the donor compartment (μg/ml) [26].

Transport across Caco-2 cell monolayers (accelerated 3-day culture method)

It has been reported that the establishment of an intact barrier with permeation functions in a serum-containing environment takes between two and four weeks for Caco-2 cells [27]. This relatively lengthy cell culturing period has led researchers to develop an advanced method that accelerates the differentiation stage of the Caco-2 cells. This method allows cells to reach enterocytic physiological characteristics within a period of only 3 days [28]. Caco-2 cells (passage between 30 and 40) were grown to a density of ≥ 250,000 cells/cm^2 prior to harvesting for seeding onto fibrillar collagen-coated 24 well inserts (1 μm pores size, 0.31 cm^2 surface area) and grown in serum free DMEM supplemented with MITO+™ Serum Extender to a density of 4 x 10^5 cells/ml for 24 h. The culture was replaced after post-seeding with serum-free Basal Seeding Medium with 500 μl Entero-STIM™ Medium on the apical side of the insert and 35 ml on the Feeder tray. Entero-STIM™ medium contains butyric acid which induces differentiation of intestinal epithelial cells *in vitro* via down regulation of *c-myc* expression [29]. The cells were maintained at 37 °C, 5% CO_2, and 90% humidity conditions for 48 h. Permeability studies were conducted with monolayers 48 h after media replacement. The same method utilised in the 21 day traditional Caco-2 cell model to measure permeation of compounds was also applied in this 3 day accelerated Caco-2 model, except that the transport was conducted on day 3.

Data analysis and statistics

Unless otherwise stated, the data are expressed as mean ± standard deviation (SD) for three experiments. Statistical data analysis was performed using a Student's t-test using Microsoft Office Excel (2007). A probability (P) value of less than or equal to 0.05 was taken as an indication of statistically significant differences.

RESULTS AND DISCUSSION

Encapsulation efficiency

The average encapsulation efficiency (EE) of the PLGA nanoparticles was 67 ± 6.0% for isoniazid. A previous study [30] has indicated that the drug loading efficiency of water soluble compounds ranged from 80 to 100% when the double emulsion solvent evaporation method was applied and a relatively high encapsulation efficiency of 79.8% was reported for mithramycin in PLGA nanoparticles prepared with this method [31]. The double emulsion solvent evaporation method seems to be specifically efficient for entrapment of hydrophilic compounds [32], which explains the relatively large encapsulation efficiency of isoniazid into PLGA nanoparticles in this study.

Surface morphology of nanoparticles

The micrographs obtained for isoniazid-encapsulated PLGA nanoparticles and Rhodamine 6G-labelled PLGA nanoparticles are depicted in Figs. **1**(A) and **1**(B), respectively. The micrographs indicate that nanoparticles with smooth surface morphology and spherical shapes with an average size of about 200 nm (indicated on a scale bar for each image) were obtained. The double emulsion solvent evaporation method utilised in this study with ethyl acetate as solvent has produced drug-loaded PLGA particles in the relatively low nanometre range, which is in agreement with previous findings [33]. Although the effect of PVA on agglomeration was not investigated in this study, the PVA in the concentration range of 1 to 8% (w/v) may have prevented agglomeration of nanoparticles as previously described [34].

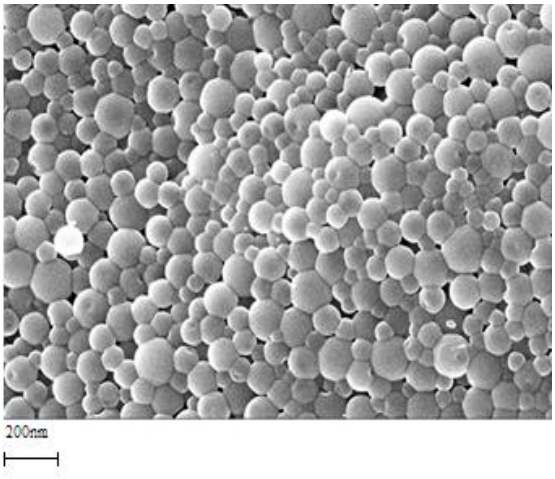

A

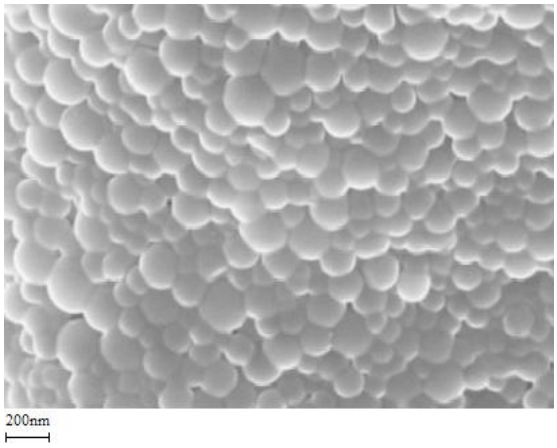

B

Fig. (1). Scanning electron micrograph of (A) isoniazid-encapsulated PLGA nanoparticles and (B) Rhodamine 6G-labelled PLGA nanoparticles (scale bar = 200 nm).

Physical characterisation of PLGA nanoparticles

The average size of the isoniazid-encapsulated and Rhodamine 6G-labelled PLGA nanoparticles as measured by means of the Zetasizer instrument were 237.9 ± 11.1 nm and 266.8 ± 10.5 nm, respectively. These average particle size values are within range to some of the particles observed with scanning electron microscopy, while a large portion of the particles are clearly below 200 nm. A previous study reported that particles with sizes in the region of 5 µm are recognized by the phagocytotic system and these particles are subjected to a clearance mechanism [35], while smaller particles and specifically those ranging from 70 nm to 200 nm are reported to escape this removal mechanism and their circulation time is thereby prolonged in the blood stream [36, 37]. A portion of the nanoparticles prepared in this study will therefore escape phagocytotic removal. Also it has been reported that particles falling within the nanometer size range can be carried through the capillary system in the blood without posing a threat of causing physical irritation to the endothelial cells or blocking the capillaries [38, 39]. Therefore the drug loaded PLGA nanoparticles formulated in this study will potentially avoid clearance by the phagocytic system and therefore may have prolonged circulation time in the systemic circulation.

A PDI value of 0.117 ± 0.022 was obtained for the isoniazid-encapsulated PLGA nanoparticles indicating a relatively high uniformity [40], which is in agreement to the value obtained from another study where PLGA particles encapsulating hydrophilic drug, doxorubicin, resulted in a PDI value of 0.158 where the particles were characterised as well dispersed and uniform [41]. The PDI value for Rhodamine 6G-labelled PLGA

nanoparticles found in this study was 0.061 ± 0.005, indicating an even narrower particle size distribution. The zeta potential of the isoniazid-encapsulated and Rhodamine 6G labelled PLGA nanoparticles in this study were found to be -21.2 ± 2.1 and -16.1 ± 1.7 mV, respectively. The negative zeta potential value could result from the free ionised carboxylic end groups of the polymer chains that are located on the surface of PLGA nanoparticles [42]. A previous study has also reported a negative zeta potential value (-18.2 mV) for PLGA nanoparticles loaded with ciprofloxacin-HCL that seemed to be uniformly dispersed in the nanoparticles [43].

Dissolution study

The percentage isoniazid released from the PLGA nanoparticles plotted as a function of time is shown in Fig. **2**. The percentage isoniazid released from the PLGA nanoparticles was relatively low over the first 4 h (only about 2% release) with a gradual increase from 8 h that reached a level just below 12% after 24 h. The initial lag phase with very low drug release is probably ascribed to the time needed for hydration of the PLGA nanoparticles to allow disentanglement of the polymer chains before the encapsulated isoniazid could be released from the nanoparticles. Interestingly, the isoniazid release from 8 h onwards appears to occur at a constant rate, but this should be investigated further over a longer period of time and appropriately modelled to be conclusive in terms of the kinetics of drug release. The isoniazid released from the nanoparticles was significantly different from the immediate release hard gelatine capsules containing pure isoniazid, which were almost completely dissolved (>80% release) within 0.5 h as evident in Fig. **2**.

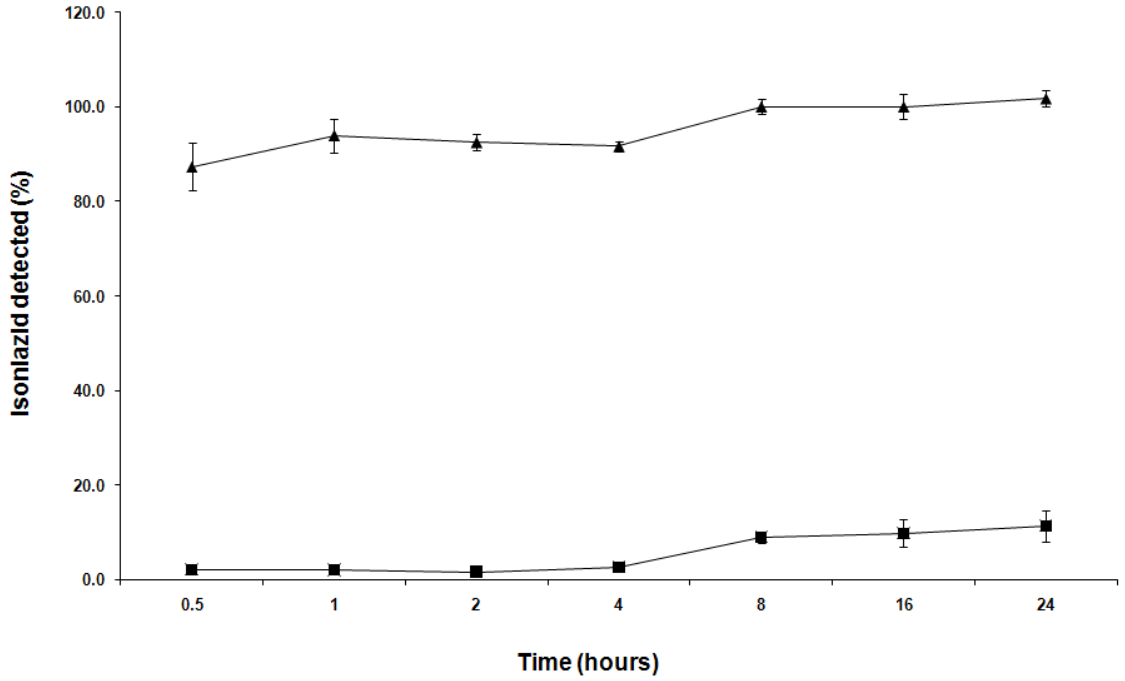

Fig. (2). Dissolution profile of isoniazid-encapsulated PLGA nanoparticles in phosphate buffer saline (pH 6.8) over a 24 h period. The relative amount of isoniazid released from nanoparticles was extrapolated from a standard curve of pure isoniazid and the results were expressed as percentage relative to initial amount of isoniazid encapsulated in PLGA (determined by encapsulation efficiency). (▲) isoniazid (control), (■) isoniazid-encapsulated PLGA nanoparticles. Data on the graph represents the mean and the error bars represent standard deviations of three replicates in two independent experiments.

Transport across artificial membrane

The effective permeability coefficient (P_e) values for isoniazid-encapsulating and Rhodamine 6G-labelled PLGA nanoparticles, pure isoniazid and pure Rhodamine 6G solutions as well as three reference compounds namely atenolol, verapamil and Lucifer yellow as determined with PAMPA are summarised in Table **1**.

Table 1: Average effective permeability coefficient values of the PAMPA transport experiment (mean ± SD), n = 3.

Compound	**P_e (10^{-6} cm/s)**
Atenolol	3.7 ± 0.01
Verapamil	27.5 ± 0.43
Isoniazid	16.15 ± 1.40

Isoniazid-encapsulated PLGA nanoparticles	Not detected
Rhodamine 6G	23.05 ± 2.0
Rhodamine-labelled PLGA nanoparticles	5.5 ± 0.98
Lucifer yellow	0.03 ± 0.01

Lucifer yellow cannot freely permeate lipophilic membrane barriers and therefore a P_e value above 1 x10^{-6} cm/s would indicate that membrane integrity was not achieved [44, 45]. In this study the P_e value of Lucifer yellow was 0.03 x 10^{-6} cm/s and the PAMPA membranes therefore exhibited good integrity. The P_e of the hydrophilic, poorly permeable drug atenolol was 3.7 x 10^{-6} cm/s, while it was 27.5 x 10^{-6} cm/s for the highly permeable drug verapamil. No transport of isoniazid from the isoniazid-encapsulating PLGA nanoparticles could be detected across the membrane of the PAMPA model after 5 h of incubation, yet isoniazid in solution did permeate to a relatively moderate extent with a P_e value of 16.15 x 10^{-6} cm/s. Interestingly, both Rhodamine 6G and Rhodamine 6G-labelled PLGA nanoparticles permeated through the membrane with P_e values of 23.05 x 10^{-6} cm/s and 5.5 x 10^{-6} cm/s, respectively. The fact that isoniazid from the isoniazid-encapsulating PLGA nanoparticles could not be detected may be explained by the slow release of this drug from the nanoparticles. Therefore, although the nanoparticles pass through the membrane (as evident from the P_e value obtained for the Rhodamine 6G-labelled nanoparticles) it was not detected in the case of the isoniazid-encapsulating PLGA nanoparticles because the isoniazid must first be released into solution before it can be detected by UV absorbance. On the other hand, detection of Rhodamine 6G-labelled PLGA nanoparticles by fluorescence is not dependent on release of the Rhodamine 6G because it can be detected while attached to the nanoparticles. The PAMPA model has certain disadvantages and is only suitable for pre-screening of drug molecules that can permeate the membrane passively and no metabolic enzymes are present.

Transport across Caco-2 cell monolayers (traditional 21 day culture method)

An average transepithelial electrical resistance (TEER) value of 250 $\Omega.cm^2$ was obtained for the Caco-2 cell monolayers at day 20, while the Lucifer yellow rejection was already 83.32 ± 0.3% at day 10 after seeding and it increased to a value of 96.88 ± 0.2% at day 21. The apparent permeability coefficient (P_{app}) values for the transport from the experimental groups and reference compounds across the traditional 21 day cultured Caco-2 cell monolayers are shown in Fig. **3**.

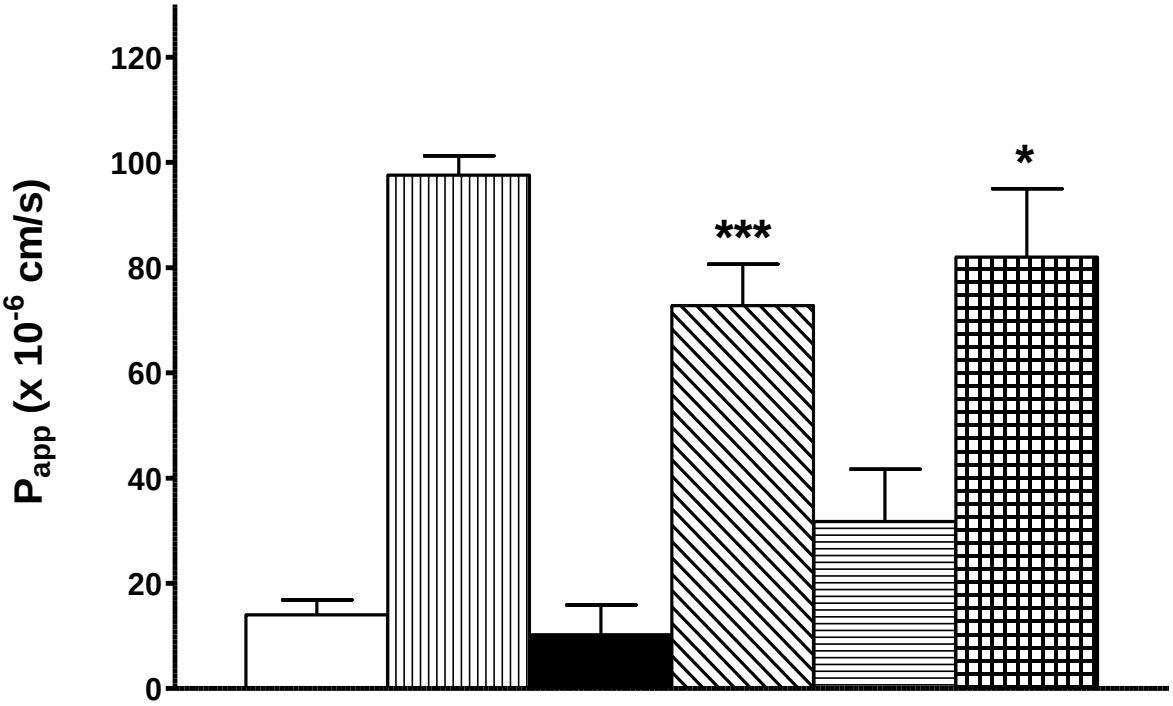

Fig. (3). Apparent permeability coefficient (P_{app}) values obtained for the transport of different compounds across the conventional 21-day Caco-2 cell model over a 24 h period. (☐) atenolol, (▥) verapamil, (■) isoniazid-encapsulated PLGA nanoparticles, (▨) isoniazid, (▤ Rhodamine 6G-labelled PLGA nanoparticles and (▦) Rhodamine 6G. Data on the graph represents the mean and the error bars represent standard deviations of three replicates in three independent experiments. Statistical comparison was amongst the experimental groups. Isoniazid permeated more adequate than isoniazid-encapsulated PLGA nanoparticles, *** P = 0.00073; Rhodamine 6G-labelled PLGA nanoparticles permeated more sufficient than isoniazid-labelled PLGA nanoparticles, (* P = 0.045), by Student's t-test: paired two samples for means.

The apparent permeability coefficient (P_{app}) values for isoniazid-encapsulating PLGA and pure isoniazid in solution were 10.2 ± 5.6 x 10^{-6} cm/s and 72.7 ± 7.8 x 10^{-6} cm/s, respectively and the difference between them was statistically significant (Fig. **3**). Permeability of isoniazid-encapsulating PLGA nanoparticles was almost similar to that of the reference compound, atenolol (14.3 ± 2.8 x 10^{-6} cm/s). The lower transport of isoniazid encapsulated in the PLGA nanoparticles as compared to the transport of the isoniazid in solution can be explained by the same argument given above, namely that the detection of the nanoparticles transport is dependent on the release of the isoniazid from the nanoparticles into solution. Therefore, although the isoniazid encapsulated PLGA nanoparticles may have permeated to a larger extent it could not be detected by means of

the indirect way of measuring the concentration of isoniazid released from the nanoparticles. The transport of Rhodamine 6G-labelled PLGA nanoparticles was therefore included in this study to measure the transport of the PLGA nanoparticles across the Caco-2 cell monolayers.

Permeability value of Rhodamine 6G-labelled was 31.7 ± 9.9 x 10^{-6} cm/s whereas for highly permeated pure Rhodamine and verapamil were 82.0 ± 13.0 x 10^{-6} cm/s and 97.6 ± 4.4 x 10^{-6} cm/s, respectively. A significant difference between isoniazid-encapsulated PLGA and Rhodamine 6G-labelled PLGA nanoparticles was noted. The results therefore indicate acceptable transport of the PLGA nanoparticles across the Caco-2 cell monolayers. The fact that the PLGA nanoparticles have been transported to a similar or higher extent than that of atenolol indicates that sufficient absorption could be expected, since although atenolol is considered a poorly permeable compound, sufficient blood levels are obtained with oral administration of atenolol.

The cell monolayer integrity didn't seem to be compromised during the transport studies since the TEER values at the end of the experiment did not change significantly from the values taken before the experiment was conducted (data not shown). This rules out the perturbation of tight junctions and ion transport properties that could possibly be induced by PLGA nanoparticles.

Transport across Caco-2 cell monolayers (accelerated 3 day culture method)

The Caco-2 cell monolayers grown by means of the 3 day accelerated method showed very good integrity with a Lucifer yellow rejection value of 98.89 ± 0.29% only 3 days post-seeding. The apparent permeability coefficient (P_{app}) values for the transport from the experimental groups and reference compounds across the accelerated 3 day cultured Caco-2 cell monolayers are shown in Fig. **4**.

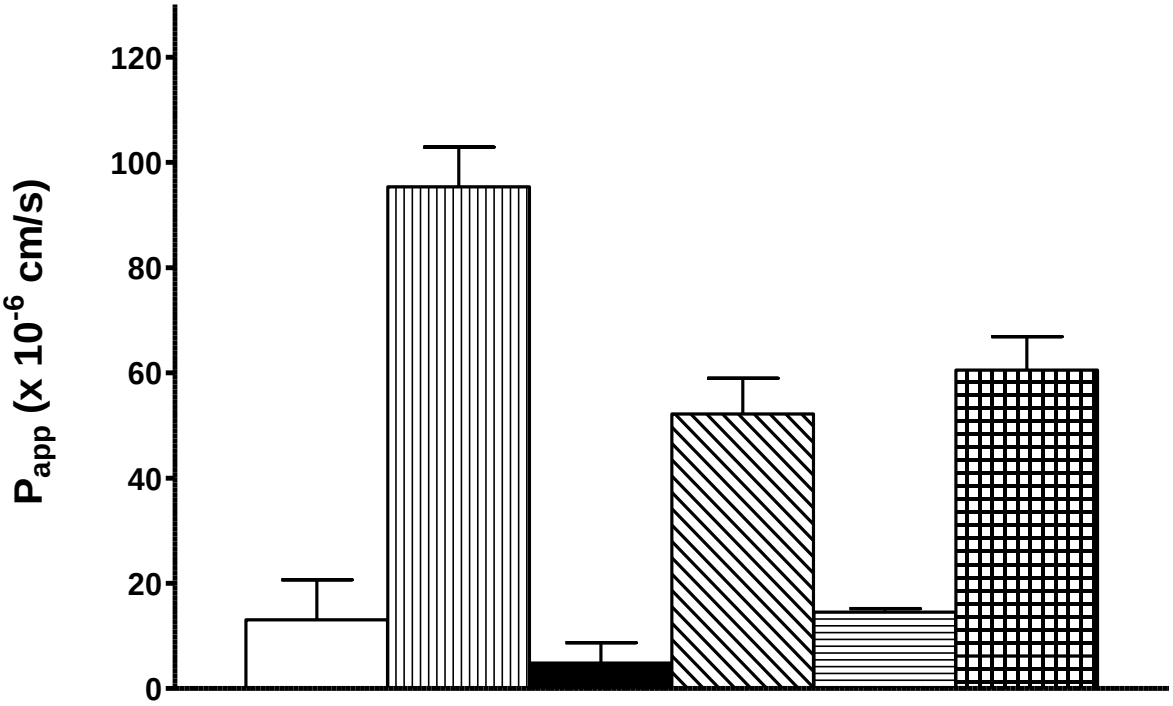

Fig. (4). Apparent permeability coefficient (P_{app}) values obtained for the transport of different compounds across the 3-day accelerated Caco-2 cell model over a 24 h period. (☐) atenolol, (◫) verapamil, (■) isoniazid-encapsulated PLGA nanoparticles, (▨) isoniazid, (▦) Rhodamine 6G and (▤) Rhodamine 6G-labelled PLGA nanoparticles. Data on the graph represents the mean and the error bars represent standard deviations of three replicates in three independent experiments. Statistical comparison was amongst the experimental groups. Pure isoniazid permeated much better than isoniazid-encapsulated PLGA nanaoparticles.

The apparent permeability coefficient (P_{app}) values for isoniazid-encapsulating PLGA and pure isoniazid in solution were 4.84 ± 3.9 x 10^{-6} cm/s and 52.12 ± 6.8 x 10^{-6} cm/s, respectively. Rhodamine 6G-labelled PLGA nanoparticles permeated to a similar extent as slowly permeable atenolol, 14.5 ± 0.7 x 10^{-6} cm/s and 13.07 ± 7.6 x 10^{-6} cm/s, respectively. Whereas pure Rhodamine 6G and highly verapamil permeability values were 60.5 ± 6.3 x 10^{-6} cm/s and 95.34 ± 10.5 x 10^{-6} cm/s, respectively. These transport results therefore confirm the transport results obtained from the traditional 21 day Caco-2 cell culture model, even though P_{app} values of 21 day method were slightly higher. Once again, the transport of the nanoparticles was similar to that of atenolol and could therefore provide acceptable absorption for systemic delivery of an encapsulated drug.

CONCLUSION

Although isoniazid-encapsulated PLGA nanoparticles have only shown permeability similar to that of the poorly permeable reference compound, atenolol, in the Caco-2 cell models, such was attributed to slow release of isoniazid from the nanoparticles. On the other hand, adequate amounts of Rhodamine 6G-labelled PLGA nanoparticles transported across permeation models used in this study which shows great potential of delivering certain drugs in a controllable manner. The permeability models used in this study (Caco-2 cell line and PAMPA) showed similar permeation trends for the nanoparticles and they are therefore suitable for permeation validation purposes. The combination of permeation models used in this study merit their usefulness in screening permeability across intestinal epithelia. The PLGA nanoparticles which permeated efficiently across epithelial membrane with release of isoniazid in a controllable manner therefore exhibits potential advantages over conventional methods for anti-TB drug delivery.

ACKNOWLEDGEMENTS

This work was funded by the Department of Science and Technology (DST) grant DMLIB-#49779-v2-MOA. Acknowledgements go to CSIR for studentship financial support.

ABBREVIATIONS

FDA = Food and Drug Administration

PAMPA = Parallel artificial membrane permeability assay

PDI = Polydispersity index

PLGA = Poly(D,L-lactide-*co*-glycolide)

PVA = Poly (vinyl alcohol)

SEM = Scanning electron microscopy

TEER = Transepithelial electrical resistance

DECLARATION OF INTEREST

The authors declare that they have no conflict of interest to disclose.

REFERENCES

[1] World Health Organisation, 2010. Global Tuberculosis Control 2011. http://www.who.int/tb/publications/global_report/en/index.html (Accessed February 10, 2012).

[2] Corbett, E.L.; Marston, B.; Churchyard, G.J.; de Cock, K.M. Tuberculosis in sub-Saharan Africa: opportunities, challenges and change in the era of antiretroviral therapy. *Lancet*, **2006**, *367*, 926-937.

[3] Onyebujoh, P.; Zumla, A.; Ribeiro, R.; Rustomjee, R.; Mwaba, P.; Gomes, M.; Grange, J. Treatment of tuberculosis: present status and future prospects. *Bull. W.H.O.*, **2005**, *83*, 857-865.

[4] Mitchison, D.A. The role of individual drugs in the chemotherapy of tuberculosis. *Int. J. Tuberc. Lung Disease*, **2000**, *4*, 796-806.

[5] Hsu, Y.Y.; Gresser, J.D.; Stewart, R.R.; Trantolo, D.J.; Lyons, C.M.; Simons, G.A.; Gangadharam, P.R.; Wise, D.L. Mechanisms of isoniazid release from poly(D,L-lactide-*co*-glycolide) matrices prepared by dry-mixing and low density polymeric foam methods. *J. Pharm. Sci*., **1996**, *85*(7), 706-713.

[6] Letendre, L.; Scott, M.; Dobson, G.; Hidalgo, I.; Bruce, A. Evaluating barriers to bioavailability *in vivo*: validation of a technique for separately assessing gastrointestinal absorption and hepatic extraction. *Pharm. Res*., **2004**, *21*(8), 1457-1462.

[7] Lee, V.H.L.; Yang, J.J. In: *Oral Drug Delivery in Drug Delivery and Targeting;* Hillery, A.M.; Lloyd, A. W.; Swarbrick, J; Ed.; Taylor and Francis: London, **2001**; pp. 145-183.

[8] Hamman, J.H.; Enslin, G.M.; Kotze, A.F. Oral delivery of peptide drugs. *BioDrugs*, **2005**, *19*, 165-177.

[9] Wacher, V.J.; Salphati, L.; Benet, L.Z. Active secretion and enterocytic drug metabolism barriers to drug absorption. *Adv. Drug Del. Rev.*, **1996**, *20*, 99-112.

[10] Balayssac, D.; Authier, N.; Cayre, A.; Coudore, F. Does inhibition of P-glycoprotein lead to drug-drug interactions? *Toxicol. Lett.*, **2005**, *156*, 319-329.

[11] Panyam, J.; Labhasetwar, V. Targeting intracellular targets. *Curr. Drug Deliv.*, **2004**, *1*, 235-247.

[12] Torchilin, V.P. Liposomes as delivery agents for medical imaging. *Mol. Med. Today*, **1996**, *2*, 242-249.

[13] Lee, R.; Huang, L. Lipidic vector systems for gene transfer. *Crit. Rev. Ther. Drug*, **1997**, *14*, 173-206.

[14] Muthu, M.S. Nanoparticles based on PLGA and its co-polymer: An overview. *Asian J. Pharm.*, **2009**, *3*, 266-273.

[15] Yadav, K.S.; Sawant, K.K. Formulation optimization of etoposide loaded PLGA nanoparticles by double factorial design and their evaluation. *Curr. Drug Deliv.*, **2010**, *7*(1), 51-64.

[16] Juni, K.; Nakano, M. Poly(hydroxy acids) in drug delivery. *Crit. Rev. Ther. Drug*, **1987**, *3*, 209-232.

[17] Gautier, S.E.; Oudega, M.; Fragoso, M.; Chapon, P.; Plant, G.W.; Bunge, M.B.; Parel, J.M. Poly(alpha-hydroxy acids) for application in the spinal cord: resorbability and biocompatibility with adult rat Schwann cells and spinal cord. *J. Biomed. Mater. Res.*, **1998**, *42*, 642-654.

[18] Zolnik, B.S.; Burgess, D.J. Effect of acidic pH on PLGA microsphere degradation and release. *J. Control. Release*, **2007**, *122*, 338-344.

[19] Hamman, J.H.; Demana, P.H.; Olivier, E.I. Targeting receptors, transporters and site of absorption to improve oral drug delivery. *Drug Target Insights*, **2007**, *2*, 71-81.

[20] Semete, B.; Booysen, L.; Lemmer, Y.; Kalombo, L.; Katata, L.; Verschoor, J.; Swai, H.S. *In vivo* evaluation of the biodistribution and safety of PLGA nanoparticles as drug delivery systems. *Nanomed. Nanotech. Biol. Med.*, **2010**, *6*, 662-671.

[21] Yang, L.; Alexandridis, P. Physicochemical aspects of drug delivery and release from polymer-based colloids. *Curr. Opin. Coll. Interface Sci.*, **2000**, *5*, 132-143.

[22] Li, J.; Volpe, D.A.; Wang, Y.; Zhang, W.; Bode, C.; Owen, A.; Hildago, I.J. Use of transporter knockdown Caco-2 cells to investigate the *in vitro* efflux of statin drugs. *Drug Metab. Dispos.*, **2011**, *39*(7), 1196-1202.

[23] Avdeef, A.; Strafford, M.; Block, E.; Balogh, M.P.; Chambliss, W.; Khan, I. Drug absorption *in vitro* model: filter-immobilized artificial membranes: 2. Studies of the permeability properties of lactones in Piper methysticum Forst. *Eur. J. Pharm. Sci.*, **2001**, *14*, 271-280.

[24] Artursson, P.; Palm, K.; Luthman, K. Caco-2 monolayers in experimental and theoretical predictions of drug transport. *Adv. Drug Deliv. Rev.*, **2001**, *46*(1-3), 27-43.

[25] Violante, G.; Zerrouk, N.; Richard, I.; Provot, G.; Chaumeil, J.C.; Arnaud, P. Evaluation of the cytotoxicity effect of dimethyl sulfoxide (DMSO) on Caco2/TC7 colon tumor cell cultures. *Biol. Pharm. Bull.*, **2002**, *25*, 1600-1603.

[26] Ho, N.F.; Burton, P.S.; Conradi, R.A.; Barsuhn, C.L. A biophysical model of passive and polarized active transport processes in Caco-2 cells: Approaches to uncoupling apical and basolateral membrane events in the intact cell. *J. Pharm. Sci.*, **1995**, *84*, 21-27.

[27] Rubas, W.; Jezyk, N.; Grass, G.M. Comparison of the permeability characteristics of a human colonic epithelial (Caco-2) cell line to colon of rabbit, monkey and dog intestine and human drug absorption. *Pharm. Res.*, **1993**, *10*, 113-118.

[28] Swiderek, M.; Mannuzza, F. Poster Presentation at FASEB Meeting, Anaheim, California. 4. Goldberger, A.; LaRocca, P.; Asa, D.; **1994**. Poster Presentation at International.

[29] Soueimani, A.; Asselin, C. Regulation of c-myc expression by sodium butyrate in the colon carcinoma cell line Caco-2. *FEBS Lett*., **1993**, 326-345.

[30] Iwata, M.; McGinity, J.W. Preparation of multi-phase microspheres of poly(D,L-lactic acid) and poly(D,L-lactic-*co*-glycolic acid) containing a W/O emulsion by a double emulsion solvent evaporation technique. *J. Microencapsul.*, **1992**, *9*, 201-214.

[31] Cohen-Sela, E.; Teitlboim, S.; Chorny, M.; Koroukhov, N.; Danenberg, H.D.; Gao, J.; Golomb, G. Single and double emulsion manufacturing techniques of an amphiphilic drug in PLGA nanoparticles: formulations of mithramycin and bioactivity. *J. Pharm. Sci.*, **2009**, *98*(4), 1452-1462.

[32] Zambaux, M.F.; Bonneaux, F.; Gref, R.; Maincent, P.; Dellacherie, E.; Alonso, M.; Labrude, P.; Vigneron, C. Influence of experimental parameters on the characteristics of poly(lactic acid) nanoparticles prepared by double emulsion method. *J. Control. Release*, **1998**, *50*, 31-40.

[33] Cohen-Sela, E.; Chorny, M.; Koroukhov, N.; Danenberg, H.D.; Golomb, G. A new double emulsion solvent diffusion technique for encapsulating hydrophilic molecules in PLGA nanoparticles. *J. Control. Release*, **2009**, *133*(2), 90-95.

[34] Scholes, P.D.; Coombes, A.G.A.; Illum, L.; Davis, S.S.; Vert, M.; Davies, M.C. The preparation of sub-200 nm poly(lactide-*co*-glycolide) microspheres for site-specific drug delivery. *J. Control. Release*, **1993**, *25*, 145-153.

[35] Owens, D.E.; Peppas, N.A. Opsonization, biodistribution and pharmacokinetics of polymeric nanoparticles. *Int. J. Pharm.*, **2006**, *307*, 93-102.

[36] Ishida, O.; Maruyama, K.; Sasaki, K.; Iwatsuru, M. Size-dependent extravasation and interstitial localization of polyethyleneglycol liposomes in solid tumor bearing mice. *Int. J. Pharm.*, **1999**, *190*, 49-56.

[37] Kong, G.; Braun, R.D.; Dewhirst, M.W. Hyperthermia enables tumor-specific nanoparticle delivery: effect of particle size. *Cancer Res.*, **2000**, *60*, 4440-4445.

[38] Hafeli, U.O.; Sweeney, S.M.; Beresford, B.A.; Sim, E.H.; Macklis, R.M. Biodegradable magnetically directed Y-90-microspheres: novel agents for targeted intracavitary radiotherapy. *J. Biomed. Mater. Res.*, **1994**, *28*, 901-908.

[39] Ramachandran, N.; Mazuruk, K. Magnetic microspheres and tissue model studies for therapeutic applications. *Ann. NY. Acad. Sci.*, **2004**, *1027*, 99-109.

[40] Beginn, U. Gradient copolymers: review. *Colloid. Polym. Sci.*, **2008**, *286*, 1465-1474.

[41] Wang, L.; Broadbelt, L.J. Factors affecting the formation of the monomer sequence along Styrene/Methyl Methacrylate gradient copolymer chains. *Macromol.*, **2009**, *42*, 8118-8128.

[42] Kocbek, P.; Obermajer, N.; Cegnar, M.; Kos, J.; Krist, J. Targeting cancer cells using PLGA nanoparticles surface modified with monoclonal antibody. *J. Control. Release*, **2007**, *120*, 18-26.

[43] Dillen, K.; Vandervoort, J.; Mooter, G.V.; Ludwig, A. Evaluation of ciprofloxacin-loaded Eudragit® RS100 or RL100/PLGA nanoparticles. *Int. J. Pharm.*, **2006**, *314*, 72-82.

[44] Bruce, J.; Nguyen, N.H.; Bulgarelli, J.P.; Kristi, O.L. The influence of donor and reservoir additives on Caco-2: permeability and secretory transport of HIV protease inhibitors and other lipophilic compounds. *Pharm. Res.*, **2000**, *17*(10), 1175-1180.

[45] Tirumalasetty, P.P.; Eley, J.G. Permeability enhancing effects of the alkylglycoside, octylglucoside on insulin permeation across epithelial membrane *in vitro*. *J. Pharm. Pharmaceut. Sci.*, **2006**, *9*(1), 32-39.